Int. J. Heat Mass Transfer. Vol. 29, No. 11, pp. 1669–1681, 1986
Printed in Great Britain

0017–9310/86 $3.00+0.00
Pergamon Journals Ltd.

Moving boundary problem: heat conduction in the solid phase of a phase-change material during melting driven by natural convection in the liquid

C. BENARD, D. GOBIN and A. ZANOLI
UA 871-CNRS—Paris VI, Campus Universitaire, Bat. 502, 91405 Orsay Cedex, France

(*Received* 24 *June* 1985 *and in final form* 29 *November* 1985)

Abstract—The purpose of this paper is to present an analysis of the melting process in a rectangular enclosure, driven by the coupling of heat conduction in the solid phase and natural convection in the melt of the phase-change material (PCM). The numerical solution of the problem which is presented here is validated by comparison with precise experimental results. Heat conduction in the solid phase is shown to significantly modify the kinetics of the melting process compared with previous studies on phase change with isothermal solid phase.

INTRODUCTION

IN RECENT years, the industrial applications of solid–liquid phase change have attracted considerable attention in the process of melting (or solidification) in enclosures. In most configurations, natural convection takes place in the liquid phase [1–3] and there is clear experimental evidence that, except at the very beginning of the process, or for very low Prandtl number materials, the melting process is controlled by convective heat transfer in the liquid phase. An increasing number of experimental and numerical studies have been performed on the coupled problem of phase change with natural convection in the melt layer [4–8]. In these studies, the solid phase is maintained at the fusion temperature and the influence of heat conduction in the solid domain is not considered. In many applications, either to control a solidification process (as in crystal growth, for instance) or to extract heat from the cold wall of the system (as in latent heat storage [9]), the solid phase is maintained at a temperature lower than the fusion temperature, and transient heat conduction in the solid phase may have considerable influence on the kinetics of the melting process. A numerical solution of this coupled problem has been proposed for the solidification of liquid metals [10]. The authors use the stream-function–vorticity formulation to solve the flow fields in the liquid phase for a limited range of Rayleigh numbers; their method leads to prohibitive computer time for Ra (based on the width of the enclosure) larger than 10^5. Another limitation of this work is that the tilt of the interface in the vertical direction is assumed to be negligible, though the results show an extremely strong curvature of the interface in the top part of the enclosure.

The purpose of the present study is to give a deeper insight into the coupling of the various physical phenomena governing the melting process with non-negligible conduction in the solid phase of the phase-change material (PCM) and in the presence of natural convection in the liquid phase. The numerical simulation of the process that is presented here provides the time evolution of the temperature fields in both phases, of the flow field in the melt and of the shape and position of the interface. The present method is able to handle situations met in latent heat storage systems, where the Rayleigh number (based on the height of the enclosure) may be as large as 10^9, while the numerical methods already available are limited to a range of moderate Ra. The numerical results are compared to the measurements obtained on a carefully designed experimental set. For this comparison to be a thorough validation of our numerical method and to enable other authors to compare their numerical results to our experimental results, detailed information is provided here on the experimental boundary conditions and on the experimental results in general.

In Fig. 1 is shown a vertical cross-section (in the y–z plane) of the rectangular enclosure containing the PCM (melting temperature T_F): the dimension in the x-direction, normal to the plane of the picture, is assumed to be large compared to the height H and the width L of the enclosure, and the process may be considered as two-dimensional in the y–z plane.

Initially, the enclosure is filled with the solid material at uniform temperature $T_0 < T_F$. At time

NOMENCLATURE

A	aspect ratio of the enclosure, H/L
c^*	dimensional position of the interface (from the hot wall)
c	dimensionless position of the interface, c^*/H
C	c^*/L
D	length of the cell in the third dimension
g	intensity of gravity
Gr	Grashof number based on H, $g\beta\,\Delta T_L H^3/\nu^2$
H	height of the enclosure
$\mathbf{j}$, $(\mathbf{k})$	unit vector in the horizontal (vertical) direction
k	thermal conductivity
k^*	ratio k_S/k_L
L	width of the enclosure
L_f	latent heat
$\mathbf{n}$	normal to the interface
$Nu_{S(L)}(z)$	local Nusselt number per unit of vertical surface, equation (13)
$\overline{Nu}_{S(L)}$	average Nusselt number $\int_0^1 Nu_{S(L)}(z)\,dz$
P	dimensionless pressure, $p^*H^2/\rho_L\nu^2$
Pr	Prandtl number of the liquid material, ν/α_L
Ra	Rayleigh number, based on H, $Gr \cdot Pr$
$\partial s/\partial t$	velocity of the interface in the $\mathbf{n}$ direction
S_L	ratio $\Delta T_S/\Delta T_L$
Ste	Stefan number, $C_{p_L} \cdot \Delta T_L/L_f$
Ste^*	Ste/ρ^*
t^*	dimensional time
t	dimensionless time, $t^*\nu/H^2$
$T_0(T_1)$	temperature of the cold (hot) vertical plate
T_F	fusion temperature of the material
$\mathbf{V}$	velocity, $\mathbf{V}^* \cdot H/\nu$
v_S	equation (16)
$y^*(z^*)$	horizontal (vertical) dimensional coordinate
$y(z)$	horizontal (vertical) dimensionless coordinate, $y^*/H\,(z^*/H)$
Y	transformation in the liquid domain, equation (6)
Y_S	transformation in the solid domain, equation (10).

Greek symbols

α	thermal diffusivity
α^*	ratio α_S/α_L
β	expansion coefficient of the melt
ΔT_L	temperature difference in the liquid, $T_1 - T_F$
ΔT_S	temperature difference in the solid, $T_F - T_0$
ν	kinematic viscosity
ρ	density
ρ^*	ratio ρ_S/ρ_L.

Subscripts S (L) refer to the solid (liquid) phase.

$t^* = 0$, the temperature of one vertical wall is raised to a value $T_1 > T_F$, while the opposite wall is maintained at the initial temperature T_0. The top and bottom walls of the enclosure are supposed to be adiabatic. An air gap is left at the top part of the enclosure to allow for the volumetric expansion of the PCM upon melting.

For $t^* > 0$, melting begins to take place near the hot plate and initially heat conduction is the only heat transfer mode. As the melt layer thickness increases with time, natural convection appears in the liquid cavity and the non-uniform heat transfer distribution along the interface causes the melting front to move faster in the top part of the enclosure, as observed in previous studies [2, 5–7, 12]. As the interface moves towards the cold plate, the temperature gradient in the solid phase increases and the melting rate decreases. Finally the melting front reaches a steady position when the heat transfer from the liquid phase is compensated by the heat transfer to the solid phase.

This process is studied in the following sections. First, the numerical method used to solve the equations of the problem is described. Then details are given on the experimental set used to validate the code, and in the last section, the comparison of experimental and numerical results is presented.

NUMERICAL SOLUTION

The numerical method used in this work has been described and successfully compared to the experiments in previous publications [11, 12] in the absence of conduction in the solid phase (melting driven only by natural convection in the melt). In this section, the method is extended to the coupling with conduction in the solid phase and the main characteristics of the method are explained below.

Hypotheses and equations

The following assumptions have been made:

1. The liquid material is an incompressible, Newtonian fluid and the Boussinesq approximation is made.
2. The process is two-dimensional.
3. The thermophysical properties of the solid and liquid phases are constant over the temperature range of interest.

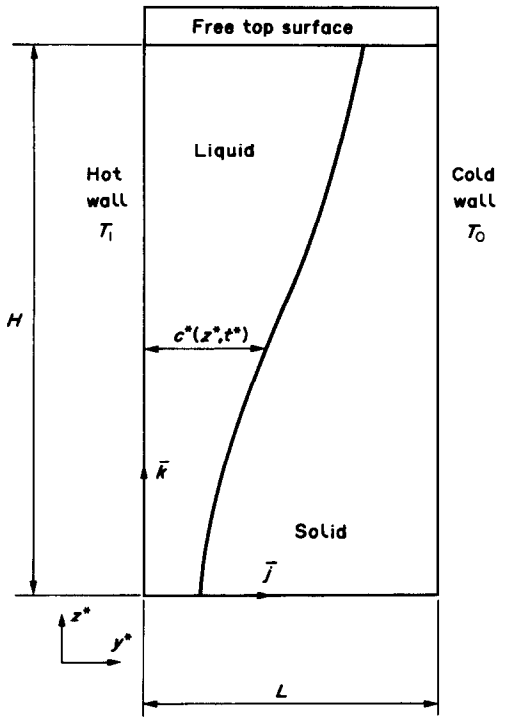

FIG. 1. Problem definition.

4. The flow in the liquid cavity is laminar.
5. The density change of the material upon melting is neglected.

The equations of natural convection in the liquid phase are then written assuming the quasi-stationarity of the melting process:

6. The convective flow is not strongly influenced by the movement of the interface. It is shown in ref. [13] that the order of magnitude of the fluid velocity in the boundary layers is $\alpha_L Ra^{1/2}/H$ and in ref. [12] that the melting front velocity in the absence of conduction in the solid phase is of the order of $\alpha_L Ste^* Ra^{1/4}/H$. The ratio of these velocities is of the order of $Ra^{1/4}/Ste^*$, which is roughly 10^3 for the range of parameters considered in our study.
7. At every time step, natural convection is in a steady state, since the characteristic time for convection to reach steady state, $t_C^* = HL/\alpha_L Ra^{1/4}$ [14, 15] is small compared to the time scale of the melting process. Indeed a lower limit of this time scale is obtained in the absence of conduction in the solid phase [12]: $t_F^* = HL/0.33\alpha_L Ste^* Ra^{1/4}$. For the range of Ste^* considered in this study ($Ste^* < 0.2$), t_F^* is one order of magnitude larger than t_C^*. Let us notice that for the range of parameters considered in this study t_C^* is of the same order of magnitude as the time required for the onset of convection in the melt layer when starting from the solid at fusion temperature: $t_0^* = 4.5H^2/\alpha_L Ste^* Ra^{1/2}$ [12]. The melting process is thus considered as a succession of quasi-static steps, a steady-state solution of the natural convection equations being calculated in a fixed liquid cavity at each step.

In the solid phase, the transient term in the conduction equation is conserved, since the characteristic time of heat diffusion is of the same order of magnitude as the time scale of the melting process.

The complete set of equations to be solved is then:

—in the liquid cavity

$$\nabla . \mathbf{V} = 0 \tag{1}$$

$$(\mathbf{V} . \nabla)\mathbf{V} = \nabla^2 \mathbf{V} - \nabla P + Gr\theta_L \mathbf{k} \tag{2}$$

$$(\mathbf{V} . \nabla)\theta_L = \frac{1}{Pr}\nabla^2 \theta_L \tag{3}$$

—in the solid domain

$$\frac{\partial \theta_S}{\partial t} = \frac{\alpha^*}{Pr}\nabla^2 \theta_S. \tag{4}$$

At the interface, the energy balance equation is:

$$(k^* S_L \nabla\theta_S - \nabla\theta_L) . \mathbf{n} = \rho^* \frac{Pr}{Ste}\frac{\partial s}{\partial t} \tag{5}$$

where $\partial s/\partial t$ is the local velocity of the melting front along $\mathbf{n}$, the normal vector to the interface. Dirichlet thermal boundary conditions are taken on the vertical walls and at the interface, and the horizontal walls are adiabatic. In the liquid cavity, the dynamic boundary condition at the top wall is taken as full slip (free surface condition), while a zero velocity condition is assumed at the other walls.

Equations (1)–(5) have been set in dimensionless form using the height H of the enclosure as the reference length and the kinematic viscosity for time and velocity. The temperature difference considered in the liquid is $T_1 - T_F$, and in the solid $T_F - T_0$. The dimensionless parameters appearing in the equations are defined in the nomenclature.

Transformation of coordinates

Liquid phase. According to the hypotheses presented above, the solution of the natural convection equations at a given time is obtained assuming that the position of the interface (the 'cold wall' of the liquid cavity) is known. As the liquid domain is non-rectangular, a transformation of coordinates is used to map the irregular physical cavity onto a rectangular computational space:

$$\left.\begin{aligned} Z &= z \\ Y &= y/C(Z) \end{aligned}\right\} \tag{6}$$

where $C(Z) = c^*(z^*)/L$ is the dimensionless position of the melting front at height z. The transformed equations are simplified by neglecting the cross terms due to the non-orthogonality of the coordinate transformation. Preliminary numerical tests have been performed for natural convection in trapezoidal and curvilinear enclosures [19] and the estimation of the neglected terms shows that the relative error on heat

fluxes at the interface is negligible if the tilt of the interface on the vertical axis and its curvature are in the range:

$$\frac{\partial c^*}{\partial z^*} < 0.3 \quad \text{and} \quad \frac{\partial^2 c^*}{\partial z^{*2}} < 0.3. \tag{7}$$

The transformation of equations (1)–(3) using (6) gives:

$$\left.\begin{aligned} \hat{\nabla}.\mathbf{V} &= 0 \\ (\mathbf{V}.\hat{\nabla})\mathbf{V} &= \hat{\nabla}^2\mathbf{V} - \hat{\nabla}P + Gr\theta_L\mathbf{k} \\ (\mathbf{V}.\hat{\nabla})\theta_L &= \frac{1}{Pr}\hat{\nabla}^2\theta_L \end{aligned}\right\} \tag{8}$$

where

$$\hat{\nabla} = \frac{1}{C(Z)}\frac{\partial}{\partial Y}\mathbf{j} + \frac{\partial}{\partial Z}\mathbf{k}, \tag{9}$$

and

$$\hat{\nabla}^2 = \frac{1}{C(Z)^2}\frac{\partial^2}{\partial Y^2} + \frac{\partial^2}{\partial Z^2}.$$

Solid phase. A similar coordinate transformation is used in the solid domain, which takes account of the moving interface: a transient solution of the heat conduction equation in the solid is desired and the interface position is then a function of both z^* and t^*. The movement of the interface leads to a deforming grid in the physical domain and introduces a convection-like term in the horizontal direction

$$Y_S = \frac{L-y^*}{H}\cdot\frac{L}{L-c^*(z^*,t^*)}. \tag{10}$$

On the other hand, the complete transformation of coordinates is kept in the solid phase. Indeed in the liquid cavity, for the rather high aspect ratios that are considered, the tilt of the interface can be mainly dealt with by a very precise approximation in the boundary-layer region, and a looser one for the bulk zone where the influence of the irregular shape is much less important. This is satisfactorily obtained with the simplified transformation already mentioned [19]. On the other hand, in the solid phase, the 'deformation' of the isotherms due to the irregular boundary is stronger and can be seen in the whole domain and the simplification of the transformed equation could affect the accuracy which is desired in the calculation of heat transfer at the interface [20]. For this reason, the coordinate transformation is not simplified in the solid phase. The transformed heat conduction equation is thus:

$$\frac{\partial\theta_S}{\partial t} - \frac{Y_S}{1-C}\frac{\partial(1-C)}{\partial t}\frac{\partial\theta_S}{\partial Y_S} = \frac{\alpha^*}{Pr}\tilde{\nabla}^2\theta_S, \tag{11}$$

with:

$$\tilde{\nabla} = \frac{1}{1-C}\frac{\partial}{\partial Y_S}\mathbf{j} + \left(\frac{\partial}{\partial Z} - \frac{Y_S}{1-C}\frac{\partial(1-C)}{\partial Z}\frac{\partial}{\partial Y_S}\right)\mathbf{k}. \tag{12}$$

Interface equation. The interface position is calculated on z = constant horizontal lines. The interface equation is thus written in terms of the horizontal velocity of the melting front, $\partial c/\partial t$ and the dimensionless heat fluxes per unit of vertical surface are introduced:

$$Nu_{L(S)}(z) = \nabla\theta_{L(S)}.\mathbf{n}\sqrt{1+\left(\frac{\partial c^*}{\partial z^*}\right)^2}. \tag{13}$$

The phase-change equation is then:

$$k^*S_L Nu_S(z) - Nu_L(z) = \rho^*\frac{Pr}{Ste}\cdot\frac{\partial c}{\partial t}. \tag{14}$$

Solution procedure

The aforementioned assumptions suggest the following method of solution:

—solve separately the natural convection equations in the fixed non-rectangular liquid cavity;
—use the steady-state temperature field in the melt to calculate the local heat transfer at the interface (liquid side);
—solve simultaneously the interface motion and the transient heat conduction equation in the solid phase on a predetermined time step.

The initialization of the calculation uses a pure conduction one-dimensional model and is terminated when the thickness of the melt layer reaches the critical value for the onset of natural convection in the liquid phase. Then, a first resolution of the convection equations is done in this initial rectangular cavity.

The numerical method uses the control volume formulation: rectangular grids are defined on the computational spaces representing the liquid and solid domains and the transformed equations are integrated over each control volume. The set of linear equations is solved using an alternate direction algorithm.

The finite-difference method used to solve the natural convection equations is based on the hybrid scheme proposed by Patankar and Spalding [16, 17]. The computational grid is generally irregularly spaced to allow a good resolution of the boundary layers near the walls without increasing the number of nodes, since the Rayleigh number for this problem may be larger than 10^9.

When a converged steady-state solution of the natural convection equations is obtained for a given liquid cavity, the local heat transfer along the interface is calculated. This distribution is considered to be constant over the time step chosen for the calculation of the interface movement and heat conduction in the solid phase. The situation is then similar to the problem studied in ref. [18]. The procedure implies that the local melting front velocity is supposed to be known when solving the conduction equation (11). Since the temperature field in the solid phase is required to solve the energy balance equation (14) which defines the

movement of the interface, an iterative procedure is used to solve the set of coupled equations (11) and (14). It should be mentioned that the 'fusion step' (the time step during which natural convection heat transfer at the interface is considered to be constant) is divided into a number of 'conduction steps' which can be taken as small as desired to ensure a good precision of the calculation of the temperature field in the solid phase. The iterative procedure for the determination of the melting front shape and position is repeated at each 'conduction step'.

At the end of a 'fusion step' a new position of the melting front is obtained as well as the time-dependent temperature field in the solid phase: the natural convection problem in the newly defined liquid cavity may be solved again. The process is repeated until the stationary position of the interface is reached. One step of the computation needs about 500 s on a UNIVAC 1110 for a 21×23 grid in the liquid cavity and a 14×20 grid in the solid domain. A complete simulation requires 15–25 fusion steps, the value of the time step being gradually increased during the melting process. The time step used for the calculation in the solid phase is of the order of 0.02 (2 min).

EXPERIMENTAL SET

The experimental device is designed to study the melting process with imposed temperature conditions on the two larger facing vertical sides of the rectangular enclosure and adiabatic horizontal and vertical terminal walls. The temperature fields in the solid and liquid phases and the interface shape and position are measured. The apparatus is conceived to provide high precision results in order to allow quantitative comparison with the numerical results obtained with the simulation code described above. Special care has thus been taken of the stability and homogeneity of the imposed boundary conditions and of the accuracy of the temperature measurements.

Description of the experimental cell

The experimental cell containing the PCM is a rectangular parallelepiped of height $H = 0.197$ m and width $L = 0.0688$ m (Fig. 2). The third dimension $D = 0.600$ m is large compared to H and L; the edge effects are thus negligible and the heat transfer is expected to be two-dimensional.

The two large vertical walls consist of metal heat exchangers through which water is circulated. The water flow path in each exchanger has been machined in a brass plate (hot wall) and in an aluminium plate (cold wall) in order to get as uniform as possible a temperature distribution on those two exchangers. The heat exchanger has been calculated for the temperature drop to be less than 0.2°C. To get rid of short term temperature fluctuations due to the regulation of the thermostats driving the cold and hot exchangers, a 0.5-m^3 well-insulated thermal bath is included in each loop (Fig. 3). In the hot wall circulation loop high

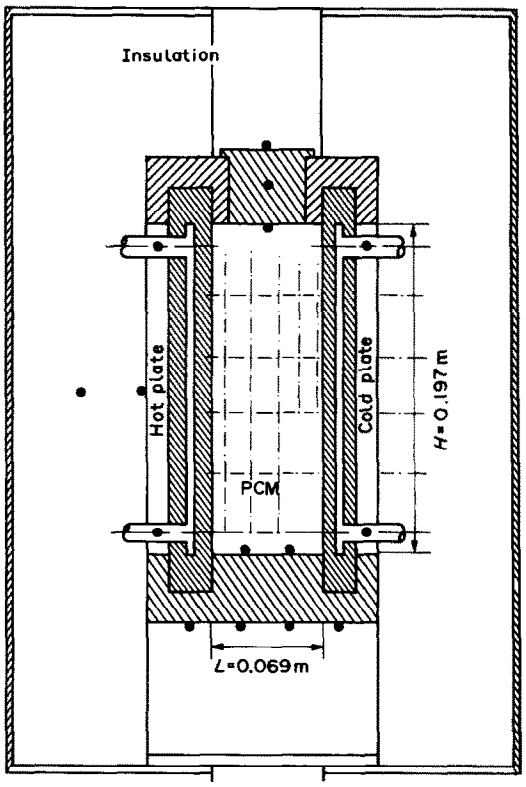

FIG. 2. Vertical cross-section of the experimental cell in the y–z plane.

rates of energy extraction are expected. To avoid effects of thermal stratification and spatial inhomogeneity in the hot thermal reservoir the water of the bath is not directly circulated in the hot wall, however, heat is extracted from the bath through a large mass heat exchanger constituting an independent inner loop in the heating system.

The four end walls are made of 0.04-cm-thick altuglass plates and the whole cell is carefully insulated with 0.08-m-thick styrofoam. The insulation of the vertical end walls is removable in order to allow the photographic observation of the melting front in the normal direction to the plane of interest.

Temperature measurements

Sixty K-type thermocouples are used to register the evolution with time of the temperatures in the system:

—0.12-mm-diameter thermocouples are located in the PCM. These thermocouples are tightened between springs along the x-direction (normal to the plane of interest) so that the junctions are located in the same vertical mid-plane, constituting a 5×5 array of regularly spaced measurement points (Fig. 4). The five horizontal levels are named A–E, from the bottom of the cell.

—At levels A, C and E, 0.12-mm-diameter thermocouples are located in the hot wall and in the boundary layer (1 and 2 mm from the plate).

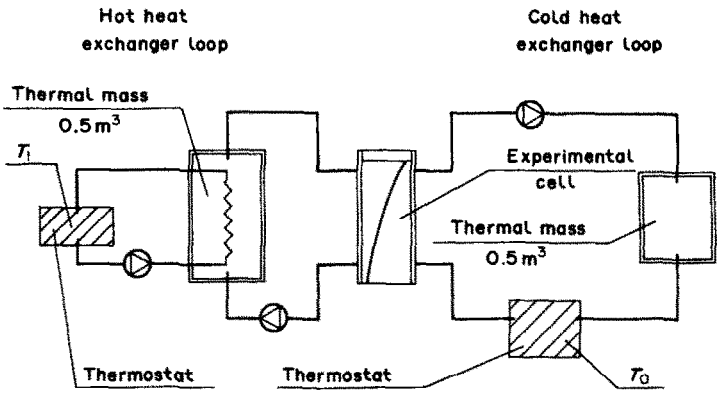

FIG. 3. Circulation loops of the experimental device.

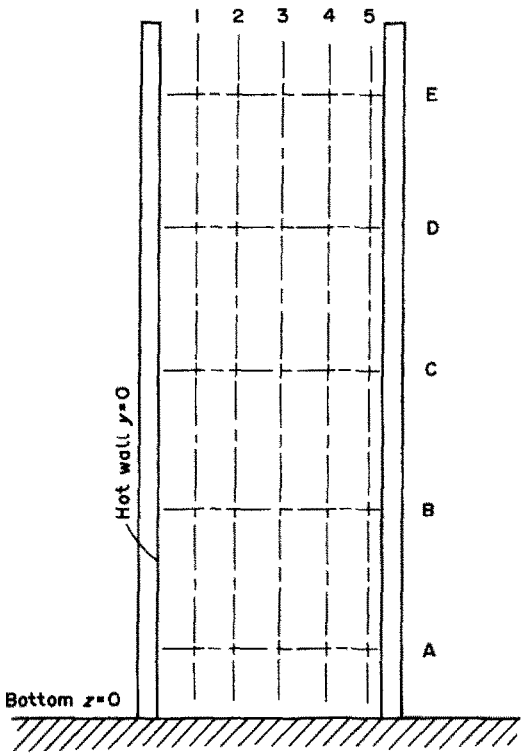

FIG. 4. Thermocouple locations in the experimental cell.

$y_1^* = 8.2 \times 10^{-3}$ m $z_A^* = 1.24 \times 10^{-2}$ m
$y_2^* = 23.3 \times 10^{-3}$ m $z_B^* = 4.71 \times 10^{-2}$ m
$y_3^* = 38.3 \times 10^{-3}$ m $z_C^* = 8.20 \times 10^{-2}$ m
$y_4^* = 53.3 \times 10^{-3}$ m $z_D^* = 11.72 \times 10^{-2}$ m
$y_5^* = 66.3 \times 10^{-3}$ m $z_E^* = 15.26 \times 10^{-2}$ m

— On the sides of the end walls, in the insulation and in the circulation loops, 0.20-mm-diameter thermocouples are used to check the stability of the temperatures and to estimate the heat losses of the cell.

The cold junctions of the thermocouples are connected to a 1-μV resolution voltmeter through a 64-channel multiplexer and the data registered is monitored by a mini-computer. The multiplexer has been placed into a thermostatted box to reduce temperature inhomogeneities on the connectors. Each channel (the thermocouple and the corresponding relay) has been individually calibrated in the temperature range of interest (10–60°C). A precision of 0.1°C on the temperature measurements could thus be reached.

Table 1. Thermophysical properties of *n*-octadecane

Thermophysical property	Temperature range	Value
Fusion temperature		28.05
Latent heat (J kg^{-1})		241000
Thermal conductivity (W m^{-1} °C^{-1})	liquid	0.157
	solid	0.390
Specific heat (J kg^{-1} °C^{-1})	liquid	2200
	solid	1900
Density (kg m^{-3})	liquid T_F	776.8
	liquid 30°C	775.5
	liquid 40°C	768.4
	solid	814
Kinematic viscosity (m^2 s^{-1})	30°C	5.005×10^{-6}
	35°C	4.468×10^{-6}
	40°C	4.013×10^{-6}

Phase-change material

The PCM to be used in such experiments must be pure and its thermophysical properties must be known with good precision. It must present good reproducibility in the repeated fusion–solidification cycles and low chemical reactivity. Among the possible candidate materials, 99.9% pure *n*-octadecane has been retained as a PCM. The thermophysical properties are reported in Table 1.

Experimental procedure

The preparatory phase of each experimental run is of great importance, since the quality of the results depends strongly on the homogeneity of the solid material and on the definition of the initial conditions. The experimental cell cannot be entirely filled in one

time with the total mass of liquid octadecane, because of the relatively large difference in density between the liquid and solid phases that would create large air cavities in the material during the solidification process. Thus, the cavity is filled by successive liquid layers, of the order of 1 cm, which are solidified before the next layer is created.

During this filling process and the following 48 h necessary to get a uniform initial temperature condition, the water of the cold loop is circulated through both the vertical walls of the enclosure: the initial condition is reached when all the thermocouples in the material indicate the same temperature within a 0.1°C margin. In the meantime, the temperature of the hot reservoir is set at the preselected value chosen for T_1 in the experiment.

At time $t^* = 0$, the cold water is extracted from the hot wall and hot water from the heating loop is circulated through the wall. The most difficult aspect of the experiment is to get the hot heat exchanger temperature to perform a reasonably well-defined step function when the experiment is started. Indeed, due to the low initial temperature necessary for the conduction in the solid to be important enough, a large $\Delta T = T_1 - T_0$ is imposed and a very strong heat flux is extracted from the heat exchanger in the first minutes of the experiment. Meanwhile the effect of the heat provided to the experimental set through the hot exchanger affects the small air gap above the PCM and also the lateral walls of the cell. As a consequence, during the first half hour of the experiment, the stability and uniformity of the boundary conditions are not perfect as shown on Fig. 9, but nevertheless, the nominal temperature of the plate is reached within 5 min to better than 5%. After that period, for a temperature step of the order of 10°C above T_F, the stability of the hot plate temperature is of the order of 0.1°C and the homogeneity is better than 0.2°C.

RESULTS AND DISCUSSION

In this section we will present and discuss the results obtained in a reference experiment, and the comparison with the numerical simulation. Initially, the experimental cell contains solid octadecane and the heat exchangers are maintained at a temperature $T_0 = 9.75$°C. At time $t^* = 0$, a temperature step of about 26°C is applied on the hot wall. During the first hour of the experiment, a transient evolution of the wall temperature is observed, due to the high rate of energy extraction from the hot plate at the beginning of the process; during the period, a 0.2°C decrease of the hot wall temperature may be noticed, before a steady value of 35.65°C is reached. In the meanwhile, the temperature of the cold wall stabilizes at 9.85°C. Under these conditions, the dimensional parameters of the experiment are:

—temperature difference in the liquid phase: $\Delta T_L = 7.60$°C

Table 2. Dimensionless parameters of the reference experiment

Parameter	Numerical value
Ra	0.846×10^9
Pr	52.14
A	2.57
Ste	0.0691
k^*	2.48
S_L	2.40
α^*	2.67
ρ^*	1.08

—temperature difference in the solid phase: $\Delta T_S = 18.20$°C

—initial height of the material: $H = 0.177$ m.

The numerical code described above has been used to simulate the experiment. The dimensionless parameters corresponding to the conditions of the experiment are reported in Table 2.

Heat transfer kinetics

The position of the melting front at different times, obtained by photographic recording (solid lines) and numerical simulation (dashed lines) is represented on Fig. 5. In a first period, the main trends of the melting process are qualitatively similar to what could be observed in previous experiments where the solid phase is kept isothermal at T_f (e.g. [2, 12]):

—conduction dominated melting at early times (the melting front is parallel to the hot plate);

—then, convection driven melting and the interface moves faster in the top part of the enclosure.

In a second period, the influence of heat extraction from the cold wall significantly modifies the evolution of the interface shape and position. Temperature gradients in the solid phase are increasing with time as the thickness of the solid material decreases. Thus, the melting process slows down and the top part of the interface does not exhibit the usual strong curvature, which is typical of the absence of conduction heat transfer in the solid phase. Then, after about 24 h, the interface reaches a stationary position.

It can be seen in Fig. 5 that the agreement of the numerical simulation with the experimental results is very good all along the process. However, the computation does not simulate the change in curvature of the interface at the very top part of the enclosure, a local discrepancy which does not depend on the grid used in the convection calculation. This difference is not due to the fact that the top thermal boundary condition, which is assumed to be adiabatic in the simulation, is disturbed in the experiment by the overflow of the liquid on the solid top surface. Indeed this phenomenon, due to the volumetric expansion of the material upon melting, has been simulated assuming that the temperature of the top surface of the solid phase is equal to the fusion temperature during a given

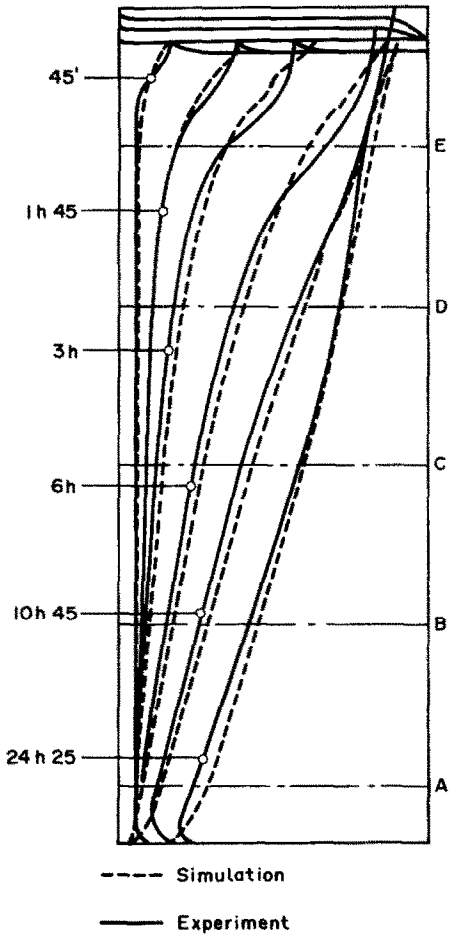

FIG. 5. Time evolution of the melting front profiles: experiment (solid lines) and simulation (dashed lines).

time. The temperature evolution in the top part of the solid is slightly affected by this disturbance, but the curvature of the interface is not sensitive to this change in the boundary condition. Thus a safe hypothesis is that this local discrepancy is due to the simplified coordinate transformation used in the natural convection calculation, since the local angle of the front with the vertical axis is higher than the maximum angle for which our approximation is valid [19]. Let us underline that the overall simulation of the melting process is not affected by this local discrepancy.

The time evolution of the distance between the hot plate and the interface may be observed with more accuracy at the different levels corresponding to the thermocouple locations (Fig. 6). Indeed the interface reaches the position of a given thermocouple when this thermocouple indicates the fusion temperature. The experimental points on Fig. 6 are obtained both from photographic recordings and from temperature measurements in the material. These curves are to be compared with the results obtained in a previous study [12] where the solid phase was kept isothermal at the fusion temperature. The experimental and numerical results have shown that as soon as a separated boundary-layer regime has been attained in the liquid phase, the local horizontal velocity of the melting front is a constant, meaning that the local Nusselt number defined by unit vertical surface [equation (13)] is constant for a given z. We have shown [12] that the only limitation for this result to be valid is that the tilt and curvature of the interface be in a given range [see equation (7)]. In the present experiment, this result is perfectly valid. Thus the time-decreasing horizontal velocity of the melting front in Fig. 6 shows the increasing influence of the heat transfer to the solid phase, which modifies the kinetics of the phenomenon.

Without getting into the detailed time evolution of local Nusselt numbers, we give in Fig. 7 the time variation of the dimensionless heat fluxes on both sides of the interface and at the cold wall, that is, of the average Nusselt numbers $\overline{Nu}_L$, $\overline{Nu}_S$ and $\overline{Nu}_0$ obtained by numerical simulation. The behavior of the Nusselt number at the interface on the liquid side, $\overline{Nu}_L$, is now well known [7, 8, 12] and it should be mentioned that the constant value reached by $\overline{Nu}_L$ when the boundary-layer regime is established verifies the correlation [12]:

$$\overline{Nu}_L = 0.33\, Ra^{1/4}. \tag{15}$$

In the solid part, the $\overline{Nu}_S$ curve, to begin with, exhibits a sharp decrease during a dimensional time interval of the order of $L^2/\alpha_S\pi^2$, meaning that the dominant phenomenon is the transient conductive regime induced in the solid phase by the temperature step. In fact, due to the rather low Stefan number, the melting front velocity is low [see equation (14)]. Thus it is not dominant in the heat transfer process as long as transient conduction is present. This can be seen more precisely by considering equation (11) and by introducing the ratio v_S between the coefficients of $\partial\theta_S/\partial Y_S$ and $\nabla^2\theta_S$ in this equation:

$$v_S = \frac{1}{\alpha_S}\cdot\frac{L^2}{L-c^*}\cdot\frac{\partial(L-c^*)}{\partial t^*}. \tag{16}$$

With the help of the experimental values of $\partial(L-c^*)/\partial t^*$, the order of magnitude of this ratio is found to be $v_S = 0.5$. Thus, if $\nabla^2\theta_S$ is important, the diffusion term will be dominant, but, when approaching the steady regime, this result indicates that the 'convective' term in (11) will rapidly become dominant. This is what appears on Fig. 7: after the initial drop, $\overline{Nu}_S$ comes to a minimum and increases progressively as the thickness of the solid domain decreases, while $\overline{Nu}_0$, the Nusselt number at the cold wall, rises slowly to the same value as $\overline{Nu}_S$, indicating that the diffusion term gets smaller and smaller. For $t^* > 5$ h, the relative difference between $\overline{Nu}_S$ and $\overline{Nu}_0$ is already less than 10%.

This sequence of an initial phase strongly dominated by transient conduction in the solid domain, followed by a phase where heat transfer is induced by the melting front movement is confirmed by the

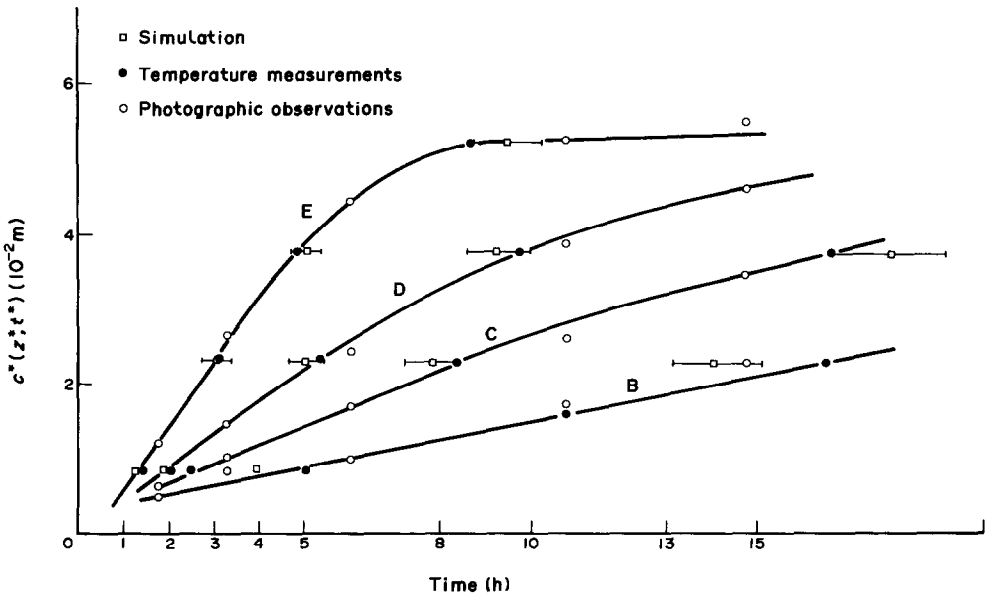

FIG. 6. Time evolution of the interface position at the thermocouples levels (B–E). □ simulation; ● experiment (thermocouple measurements); ○ experiment (photographic observation).

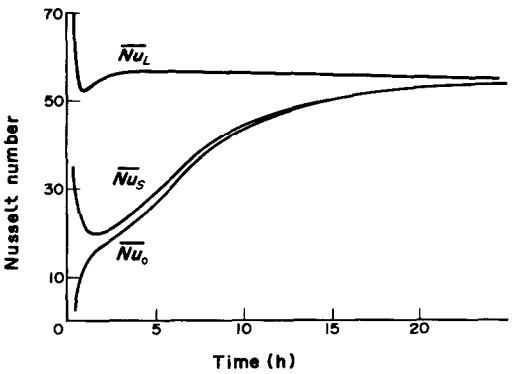

FIG. 7. Average Nusselt number evolution at the interface ($\overline{Nu}_L$, $\overline{Nu}_S$), and at the cold wall of the cell ($\overline{Nu}_0$): numerical results.

detailed analysis of the temperature field in the solid presented in the next section.

Temperature evolution in the material

The time evolution of the temperature of the thermocouples located at level D is given for a 12-h period (Fig. 8). In the solid phase, we notice that the first 2 h are characterized by a strong transient increase due to the temperature step on the hot wall. Then the evolution is slower; nevertheless, the temperature at a given point still increases as long as the thickness of the solid domain at this level is getting smaller.

It is interesting to notice by comparing the temperatures on the same vertical line (Fig. 9) that the heat transfer becomes significantly two-dimensional only after 1–1.5 h, that is, after the strong initial transient has vanished. The temperature evolution in the solid is then driven by the two-dimensional movement of the interface.

When a thermocouple is reached by the melting front and enters the liquid phase, its behaviour is exactly the same as in the classical isothermal solid experiments; its temperature increases again sharply while it crosses the thermal boundary layer along the interface, and after a maximum in the inversion zone, the temperature reaches a constant value corresponding to the stratification zone. The neighbouring thermocouples of the same level reach the same stable value after a similar evolution.

Temperature fields

The good agreement between the experimental and numerical results concerning the heat transfer balance at the interface (melting profiles, Fig. 5) is confirmed by the comparison of the temperature fields in the liquid and the solid phases.

Liquid phase. Figure 10 presents the temperature distribution in the liquid phase at three levels (B, C and D) at time $t^* = 22.5$ h. On the figure, the abscissa of the point at the fusion temperature ($\theta_L = 0$) is not the same for the different levels, since it depends on the local thickness of the liquid cavity. Because of the high Rayleigh number, the boundary layers are very thin and all the experimental points are located in the stratification zone. In this region, the numerical simulation is in very good agreement with the measurements, although a rather coarse grid is used in the central part of the cavity.

Solid phase. In the solid phase, the temperature distribution is given at three different times for level C (Fig. 11a) and level E (Fig. 11b). The calculation

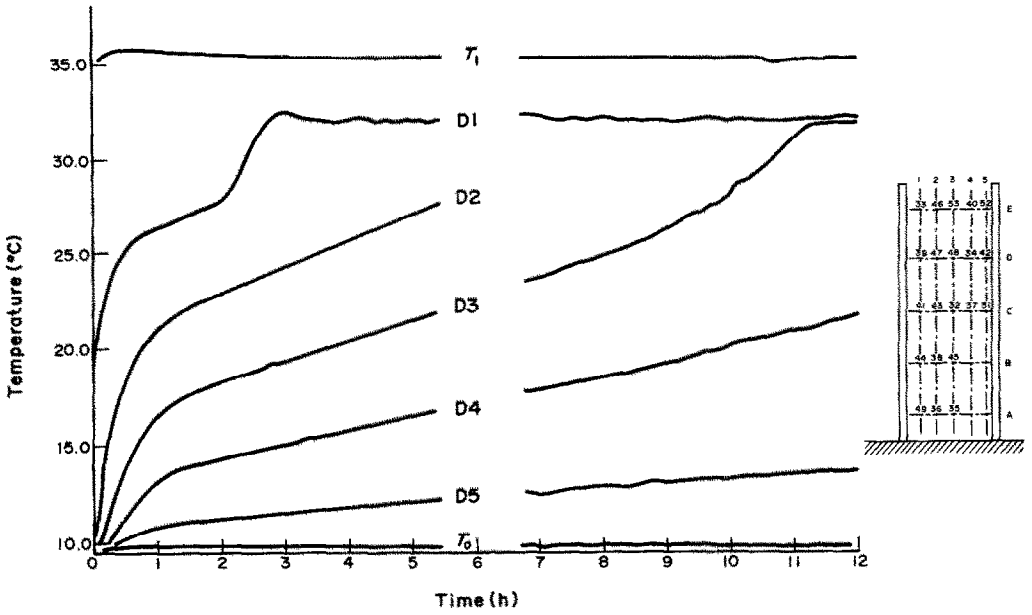

FIG. 8. Temperature evolution of the thermocouples located at level D and at the vertical walls of the cell.

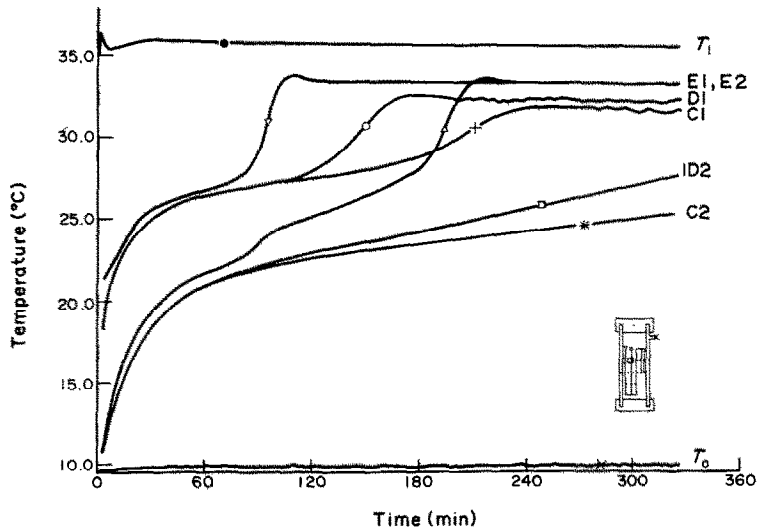

FIG. 9. Temperature evolution of the thermocouples located on lines 1 and 2 (horizontal levels C, D and E).

again gives an excellent simulation of the experimental measurements, even in this phase of the process, which is characterized by a strongly transient evolution of the temperature field in the solid phase. The local discrepancy found at the upper level (E) at $t^* = 44$ min is due to a sudden change in the upper thermal boundary condition in the experiment. Indeed the volumetric expansion of the material upon melting causes the liquid to flow from time to time over the surface of the solid phase, and the top boundary condition is not adiabatic. The influence of this perturbation is limited to the upper part of the solid domain, and it can be seen that the temperature distribution at mid-height (level C) is not affected by this phenomenon.

It is worth noticing that the numerical and experimental temperature distributions in the solid phase are almost linear at time $t^* = 2$ h. This confirms that the transient response of the solid phase due to the temperature step almost reaches a quasi-steady regime in 2 h, and that afterwards the temperature distribution remains linear, the increase of the heat flux being mainly due to the movement of the interface.

The simulated time evolution of the temperature fields in both phases is illustrated on the isotherms plotted on Fig. 12. The left part of the figure (Fig. 12a) gives the isotherms at the beginning of the melting process ($t^* = 35$ min). It appears clearly on the figure that the conduction regime is still dominant in the liquid cavity. In the solid domain, the shorter

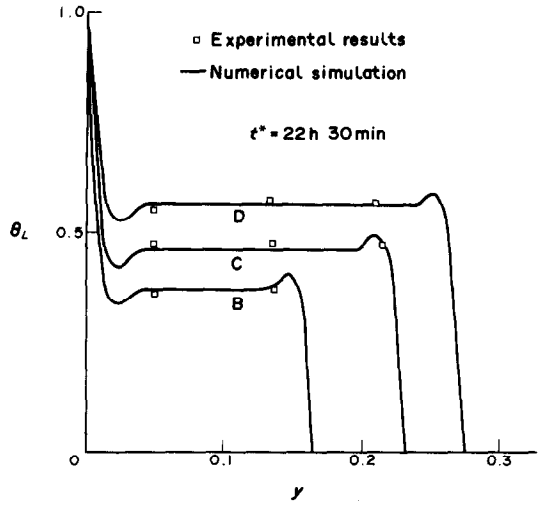

FIG. 10. Temperature profiles in the liquid phase at levels B, C, D. —— Simulation; □ measurements. Because of the irregular shape of the interface, the abscissa of the $\theta_L = 0$ point (the fusion temperature) is smaller at the lower levels.

distance between the isotherms near the interface indicates the transient regime in this phase. The isotherms plotted on Fig. 12b correspond to a later time ($t^* = 10$ h): it may be seen that the boundary layer regime is fully developed in most parts of the liquid cavity. In the solid phase, the isotherms are equally spaced, showing that the quasi-steady regime has been reached.

CONCLUSION

The very good agreement of the numerical results with careful and precise experimental measurements presented in this study show that the hypotheses used in the numerical simulation are valid for the range of parameters considered in this work ($Ra = 10^9$, $Pr = 50$, $Ste < 0.2$). These orders of magnitude are typical of applications of phase change to latent heat storage in closed rectangular cells. Under these conditions, several hypotheses have been verified:

- The natural convection flow in the liquid phase is laminar.
- The thermophysical properties of both the liquid and the solid phases may be considered to be constant, and the interface may be taken as a smooth surface.
- As far as convection in the melt is concerned, the quasi-stationarity of the melting process allowed by hypotheses 6 and 7 is a good approximation. This can be extended to all the cases where the duration of transient natural convection is negligible (hypothesis 7) as well as the effect of the interface velocity on the dynamic boundary layer (hypothesis 6). As shown earlier, this latter approximation is correct if the inequality:

$$Ra^{1/4}/Ste^* \gg 1$$

is satisfied. A sufficient condition for hypothesis 7 to be fulfilled is that

$$0.33 Ste^* \ll 1.$$

- The boundary-layer regime in the liquid cavity is dominant over the major part of the melting process. This is due to the fact that the ratio of the characteristic time for the separation of the boundary layers to the time scale of the melting process is very low in the case under consideration. Indeed the maximum value of this ratio (obtained

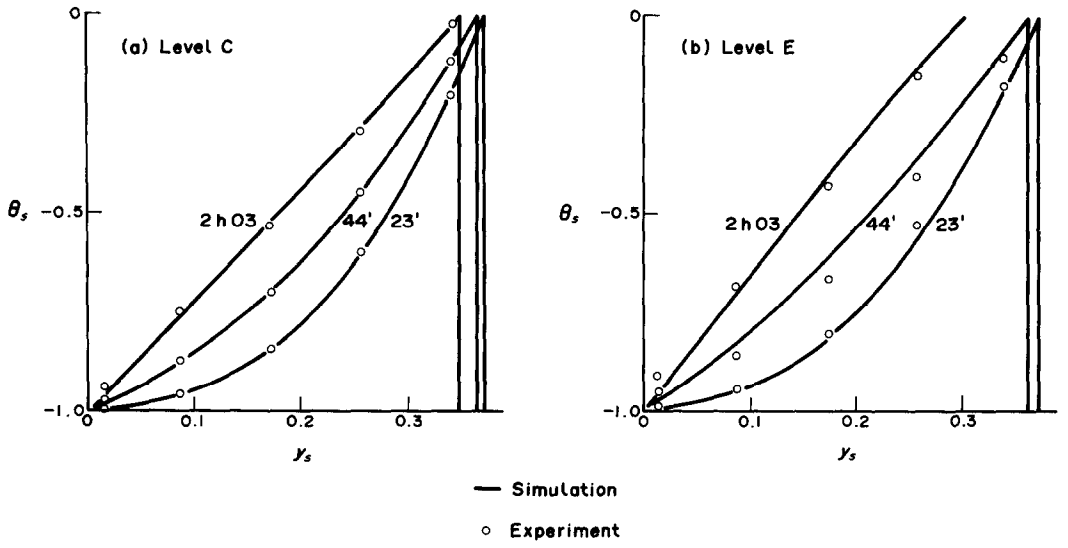

FIG. 11. Temperature profiles in the solid phase at different times: (a) level C; (b) level E. —— Simulation; ○ measurements. y_S is measured from the cold plate, thus the abscissa of the $\theta_S = 0$ point (the fusion temperature) is decreasing with time since the thickness of the solid domain is getting smaller.

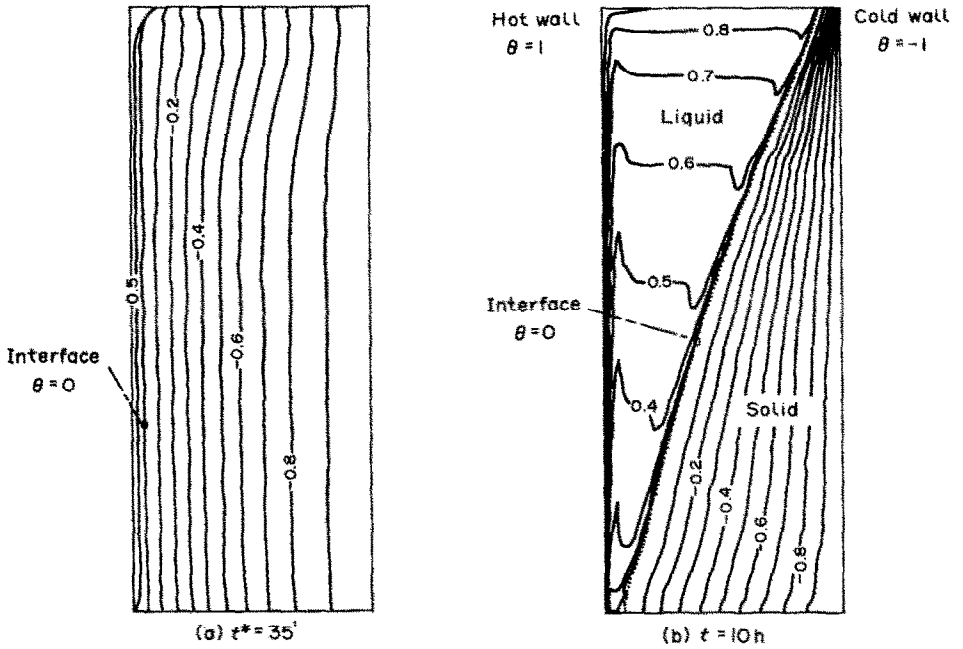

FIG. 12. Isotherm plots in the solid and liquid phases: (a) $t^* = 35$ min; (b) $t^* = 10$ h.

in the absence of conduction in the solid phase [12]) is given by:

$$t_0^*/t_F^* = 1.5A/Ra^{1/4}$$

a quantity which is much smaller than 1. Because of this situation, the well-known correlations [12, 19] giving the local heat flux at the walls of a rectangular cavity for internal natural convection in the laminar regime can be used in our problem, as long as the tilt of the melting front on the vertical axis is small.

In the solid phase, the kinetics of the system are mainly determined by the value of the parameter v_S [equation (16)], the ratio of the interface velocity to the diffusion velocity. In the case under study, the value of v_S, very close to 1, allows the definition of two successive steps: the first one dominated by conduction in the solid; and the second one by the movement of the interface.

One of the main extensions to this study will be to cover a wider range of dimensionless parameters, corresponding to other applications of phase change, and to determine the domain of validity of the preceding results.

Acknowledgements—The present work was supported by SPI Direction of CNRS and PIRSEM Research Program (ATP 'Thermique du Bâtiment'). The authors wish to thank Dr A. Gadgil for his valuable advice and comments. The computations were carried out on the UNIVAC 1110 at the PSI computer center, Université d'Orsay.

REFERENCES

1. E. M. Sparrow, R. R. Schmidt and J. W. Ramsey, Experiments on the role of natural convection in the melting of solids, *J. Heat Transfer* **100**, 11–16 (1978).
2. P. D. Van Buren and R. Viskanta, Interferometric measurement of heat transfer during melting from a vertical surface, *Int. J. Heat Mass Transfer* **23**, 568–571 (1980).
3. A. G. Bathelt, R. Viskanta and W. Leidenfrost, An experimental investigation of natural convection in the melted region around a heated horizontal cylinder, *J. Fluid Mech.* **90**, 227–239 (1979).
4. E. M. Sparrow, S. V. Patankar and S. Ramadhyani, Analysis of melting in the presence of natural convection in the melt region, *J. Heat Transfer* **99**, 520–526 (1977).
5. C. J. Ho and R. Viskanta, Heat transfer during melting from an isothermal vertical wall, *J. Heat Transfer* **106**, 12–19 (1984).
6. D. Gobin, C. Benard and A. Gadgil, Transient phase change in two dimensions coupled with convection in the liquid phase: experiments and numerical simulations, Int. Conf. on Numerical Methods for Transient and Coupled Problems, Venice, pp. 60–69 (1984).
7. M. Okada, Analysis of heat transfer during melting from a vertical wall, *Int. J. Heat Mass Transfer* **27**, 2057–2066 (1984).
8. M. Bareiss and H. Beer, Experimental investigation of melting heat transfer with regard to different geometrical arrangements, *Int. Commun. Heat Mass Transfer* **11**, 323–333 (1984).
9. C. Bénard, Y. Body and A. Zanoli, Experimental comparison of latent and sensible heat thermal walls, *Sol. Energy* **34**, 475–487 (1985).
10. R. Ramachandran, J. P. Gupta and Y. Jaluria, Two-dimensional solidification with natural convection in the melt and convective and radiative boundary conditions, *Numer. Heat Transfer* **4**, 469–484 (1981).
11. A. Gadgil and D. Gobin, Analysis of two-dimensional melting in rectangular enclosures in presence of convection, *J. Heat Transfer* **106**, 20–26 (1984).

12. C. Bénard, D. Gobin and F. Martinez, Melting in rectangular enclosures: experiments and numerical simulations, *J. Heat Transfer* **107,** 794–803 (1985).
13. A. E. Gill, The boundary-layer regime for convection in a rectangular cavity, *J. Fluid Mech.* **26,** 515–536 (1966).
14. J. Patterson and J. Imberger, Unsteady natural convection in a rectangular cavity, *J. Fluid Mech.* **100,** 65–86 (1980).
15. G. N. Ivey, Experiments on transient natural convection in a cavity, *J. Fluid Mech.* **144,** 389–401 (1984).
16. A. Gadgil, On convective heat transfer in building energy analysis. Ph.D. thesis, University of California, Berkeley, CA (1979).
17. S. V. Patankar, *Numerical Heat Transfer and Fluid Flow*. Hemisphere, McGraw-Hill, New York (1980).
18. C. F. Hsu, E. M. Sparrow and S. V. Patankar, Numerical solution of moving boundary problems by boundary immobilization and a control volume based finite difference scheme, *Int. J. Heat Mass Transfer* **24,** 1335–1342 (1981).
19. D. Gobin, Changement d'état solide–liquide: évolution temporelle du couplage entre la convection naturelle dans la phase liquide et la conduction dans la phase solide. Thèse d'Etat, Université Paris VI (1984).
20. A. Zanoli, Stockage thermique par chaleur latente: couplage de la conduction dans la phase solide avec le déplacement de l'interface et la convection naturelle dans la phase liquide. Thèse de Docteur-Ingénieur, Université Paris VI (1984).

PROBLEME DE FRONTIERE MOBILE: CONDUCTION DANS LA PHASE SOLIDE D'UN MATERIAU A CHANGEMENT DE PHASE LORS DU PROCESSUS DE FUSION COMMANDE PAR LA CONVECTION NATURELLE DANS LE LIQUIDE

Résumé—Le but de cette étude est de présenter une analyse du changement d'état solide–liquide en géometrie rectangulaire où la fusion résulte du couplage entre la conduction dans le matériau solide et la convection naturelle dans la phase liquide. La méthode de résolution numérique du problème est validée par comparaison avec des résultats expérimentaux précis. On montre en particulier l'influence de la conduction dans le solide sur la cinétique de fusion, par rapport à des études antérieures où la phase solide est maintenue isotherme.

WÄRMELEITUNG IN DER FESTEN PHASE EINES LATENTSPEICHERMATERIALS BEIM SCHMELZEN INFOLGE NATÜRLICHER KONVEKTION IN DER FLÜSSIGKEIT

Zusammenfassung—Dieser Beitrag stellt eine Untersuchung des durch die Überlagerung von Wärmeleitung im Festkörper und natürliche Konvektion in der Schmelze erzeugten Schmelzprozesses in einem rechteckigen Hohlraum vor. Die hier vorgestellte numerische Lösung des Problems wird durch einen Vergleich mit exakten experimentellen Ergebnissen bestätigt. Verglichen mit Studien über Phasenwechsel an einem isothermen Festkörper zeigt sich hier, daß die Wärmeleitung im Festkörper die Kinetik des Schmelzprozesses nachhaltig beeinflußt.

ЗАДАЧА С ПОДВИЖНОЙ ГРАНИЦЕЙ: ТЕПЛОПРОВОДНОСТЬ ТВЕРДОЙ ФАЗЫ ПРИ ПЛАВЛЕНИИ МАТЕРИАЛА, ЕСТЕСТВЕННАЯ КОНВЕКЦИЯ В ЖИДКОСТИ

Аннотация—Представлен анализ процесса плавления в прямоугольных полостях с учетом теплопроводности в твердой фазе и естественной конвекции в расплаве при фазовом изменении в материале. Представленное численное решение задачи обосновывается с помощью сравнения с точными экспериментальными результатами. Показано, что учет теплопроводности в твердой фазе существенно улучшает описание кинетики процесса плавления в сравнении с предыдущими исследованиями в предположении изотермичности твердой фазы.